PROCEEDINGS OF SPIE

SPIEDigitalLibrary.org/conference-proceedings-of-spie

Robust and objective automatic optical surface inspection using modulated dark field phasing illumination

Heejoo Choi, John Kam, Joel D. Berkson, Logan R. Graves, Huang Lei, et al.

Heejoo Choi, John Kam, Joel D. Berkson, Logan R. Graves, Huang Lei, Dae Wook Kim, "Robust and objective automatic optical surface inspection using modulated dark field phasing illumination," Proc. SPIE 11102, Applied Optical Metrology III, 1110207 (3 September 2019); doi: 10.1117/12.2529869

SPIE.

Event: SPIE Optical Engineering + Applications, 2019, San Diego, California, United States

Robust and objective automatic optical surface inspection using modulated dark field phasing illumination

Heejoo Choi[1], John Kam[1], Joel D. Berkson[1], Logan R. Graves[1], Huang Lei[2], and Dae Wook Kim*[1,3]

[1]James C. Wyant College of Optical Sciences, The Univ. of Arizona, Tucson, AZ, USA 85721
[2]State Key Laboratory of Precision Measurement Technology and Instruments, Department of Precision Instrument, Tsinghua University, Beijing 100084, China
[3]Department of Astronomy, University of Arizona, Tucson, AZ 85721, USA

ABSTRACT

Dark field illumination (DFI) is an elegant inspection technique sometimes used to detect particles on a specular surface. However, traditional DFI struggles with repeatability, limiting its applications in automated inspection. We present an improvement to DFI by introducing a modulated dark field illumination (MDFI) that utilizes the phase rather than the intensity in the detection of defects. For modulated dark field illumination (MDFI), the phase-based information is independent from the reflectance of the surface, but has a higher sensitivity to the light scattered from a defect than DFI. As a result, we obtain a robust computational image process method that is insensitive to the environment and provides clearly defined defect information. In order to extend the application to industry, the instantaneous MDFI systems were developed and validated.

Keywords: Automatic optical inspection, Particle detection, Dark field, Phase measurement.

1. INTRODUCTION

Most of the cutting-edge fabrication line requires that the substrate should be clean and without defects on the surface for successful optical lithography and other fine processes. The technologies being developed to inspect the manufacturing of products such as semiconductors and display panels is known as Automatic Optical Inspection (AOI). The AOI should have reliable, accuracy and repeatability to meet industry demands. [1-3]

One of the classical methods of surface inspection is dark field illumination (DFI) [4-8]. This method is mainly used for particle detection and defect inspection on a specular and/or transparent surface. The images are acquired by illuminating the specular surface at a grazing angle. The camera takes an image from near the surface normal where the specularly reflected light will not enter the sensor but light scattered from the particle or defect may. A DFI measurement shows high contrast images which have bright spots at the particle and/or defect and almost zero signal from the specular surface [5, 6]. Another application of DFI is called side stream illumination in microscopy. Under the microscope, by using a large incidence angle for the light, DFI creates a high contrast image between transparent (non-scattering area) and opaque objects (scattering area) [4, 7, 8].

The original DFI method relies on intensity variation to detect the defect. However, intensity-based information is easily disturbed by the environment (e.g., room light) and background reflectance (e.g., mask pattern or varying material deposition) while the phase information is insensitive to these intensity fluctuations from environments. In this paper, we propose modulated DFI (MDFI), which uses modulated illumination to utilize phase information to more reliably detect defects [9]. We will first introduce the phase based DFI (Chap. 2) and then study the diverse possibilities of the recorded phase needed to produce high contrast data (Chap. 3). The improved consistency of MDFI over the traditional DFI makes it more suitable for AOI (Chap. 4). Additionally, in Chap. 5, we developed an instantaneous modulated dark field (iMDFI) using color multiplexing and the inspection performances were investigated.

Applied Optical Metrology III, edited by Erik Novak, James D. Trolinger, Proc. of SPIE Vol. 11102, 1110207 · © 2019 SPIE · CCC code: 0277-786X/19/$21 · doi: 10.1117/12.2529869

2. MODULATED DARK FIELD ILLUMINATION (MDFI)

2.1 System configuration

The traditional DFI uses a source with a large incident angle to induce the intensity variations from defects. While turning the source off and on, the light scattered from the defects change with the same phase as the grazing light source, but the back ground does not change the brightness. The difference (or subtraction) of the images taken with the source off and on shows the defects which are clearly distinguishable against the back ground. However, if there are intensity variations by an undesirable input (e.g., room light, mask pattern) then the subtracted map may show these effects as well. In the worst case the perturbed signal may wash out the signal from the surface defect. (Fig 3.) To resolve the above controversy, an intensity independent method is developed.

The system layout is the same as traditional DFI, except for the addition of a monitor (Fig. 1). In order to plate a signal to the background surface (specular), the monitor is installed normal to the sample. Now, instead of seeing a variation in intensity from only the defect, the two signals are measured 1) scattering light from the defect (from LED), 2) specular reflection from background (from monitor).

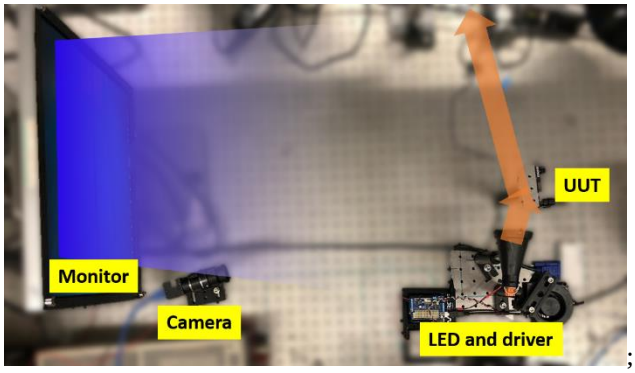

;

Figure 1. Setup picture of MDFI. The orange arrow represents the direction of the grazing angle illumination of LED.

The important difference of this proposed method is producing a correct time varying signal from each source. For instance, we could use a time dependent sine and cosine intensity for the LED and monitor respectively. In these initial conditions, the scattered light and background signal have a π phase shifted signal. The advantage of this method is shown in Fig. 2

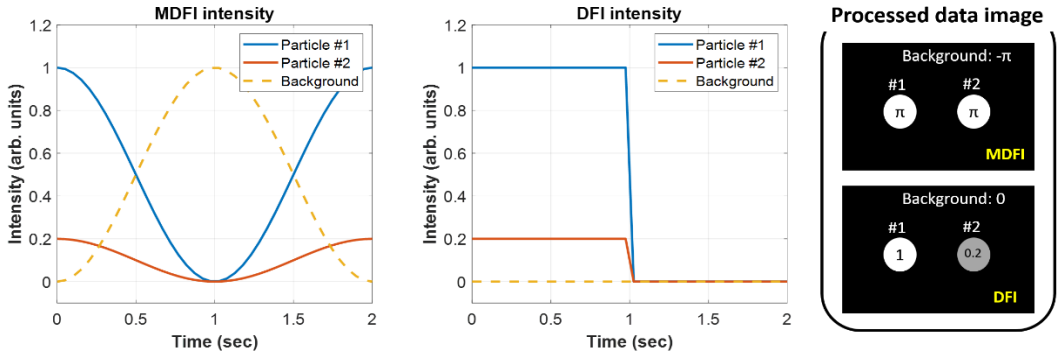

Figure 2. A time varying intensity plot and the result of data calculation. Particles #1 and #2 represent the strong and weak signal from defects, respectively. MDFI has the same signal strength for both particles while DFI has the intensity dependent signal ratio. If a certain threshold is set to judge a defect (e.g., 0.5 for DFI), #2 particle might be incorrectly dismissed.

As shown in Fig. 2 the phase-based information provides a high contrast inspection result even when the signal from the defect is smaller than the nominal defect. In the case of the chrome patterned substrate, as you can find at Fig. 3, the deposition of the different material induces the reflectance variation. Because the DFI inspects based on intensity, the

reflectance changes of the patterns introduce false positives. Meanwhile, MDFI isn't affected by the pattern on the substrate because the pattern (specular, less reflectance) and the background (specular, high reflectance) have the same phase which is clearly distinguishable against the signal from the defect (scattered).

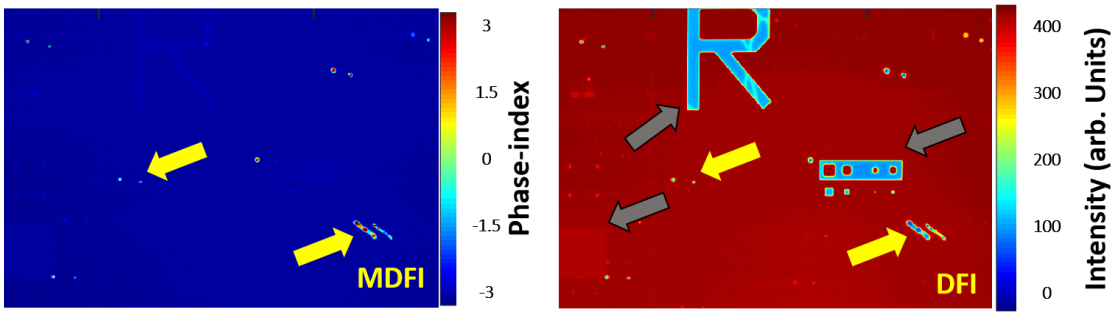

Figure 3. The test result of the patterned substrate. The yellow and grey arrow points out the defect and mask pattern, respectively. In the MDFI results, the mask pattern makes a significantly weaker signal than the defect. However, in the DFI test, the pattern shows almost similar signal as a defect, so it's not easy to provide the clear judgment of defect existing.

2.2 Survey the best phase steps

The phase for both light sources is the key factor of MDFI data quality. If the phase contrast is too small, the output data will show inconclusive results similar to DFI. In order to have the best phase contrast result, we examined the proper phase steps (difference) for both light sources. Because we drive each light source individually they may be any phase step we'd like within the hardware capabilities (e.g., the sensitivity of camera sensor, gray scale of the monitor, and LED driver).

The well-known method of phase retrieval is done by taking the arctangent of the signal variation. The recorded intensity for every pixel is calculated using Eq. 1. The *N* is the total phase steps and x and y are the pixel coordinates. *I* is the recorded signal at *n-th* phase steps. From this inverse tangent calculation, the pixel of background will have the same phase from the monitor and the pixel pertaining of the particle (defect) will have the phase associated with the LED. If the camera system had an infinite lateral resolution, the boundary of the particle would be resolved perfectly and no pixel would record a phase that was a linear combination of the two input signals. However, in practice images of the particles will have a blurred boundary due to the finite size of sensor's pixels, so the recorded intensity at these pixels will be sum of the monitor (background) and LED (particle) signal. In the case that the inspection target is smaller than the camera resolution, MDFI might record the mixed signal from both sources. The conditions which occur when a particle boundary lies within the scene of a pixel is simulated using Eq. 1, 2 and 3.

$$\Phi_{index}(x,y) = atan\left(\frac{\sum_{n=1}^{N} I(x,y,n)sin\left(\frac{2\pi n}{N}\right)}{\sum_{n=1}^{N} I(x,y,n)cos\left(\frac{2\pi n}{N}\right)}\right) \quad (1)$$

$$I_{particle}(x,y,n) = A_1(x,y)sin\left(\frac{\pi n}{N} + \Phi_1\right) \quad (2)$$

$$I_{background}(x,y,n) = A_2(x,y)sin\left(\frac{\pi n}{N} + \Phi_2\right) \quad (3)$$

Where $I_{particle}$ is the intensity from light scattered by particle and $I_{background}$ is the intensity reflected by the specular surface. A_1 and A_2 are the fill factors of each signal which takes into account a combined recorded intensity. Φ_1 and Φ_2 are the initial broadcasted phase values needed to create a distinguishable phase map. If we used the normal inverse arctan calculation, the result is naturally bound within $-\pi/2$ to $\pi/2$ because it cannot recognize the sign of the numerator and denominator. On the other hand, the four-quadrant inverse tangent considers the sign of the numerator and denominator and can extend the range to $\pm\pi$.

Using the above Equations and four-quadrant inverse tangent, we survey the best phase steps for LED (Φ_1) and monitor (Φ_2). The below table shows the representative cases.

Table 1. The representative phase cases

	Case 1	Case 2	Case 3	Case 4
Φ_1	–π/4	0	0	π/2
Φ_2	π/4	π/2	π	–π/2
$\lvert \Phi_1 - \Phi_2 \rvert$	π/2	π/2	π	π

With the infinite phase possibilities of Φ_1 and Φ_2, it is necessary to determine the correct combinations which offer good contrast. The first condition that must be met is a clear contrast at the full fill factor (e.g., $A_1 = 1$, $A_2 = 0$) condition. Additionally, the decomposed contrast must be maximized in the mixed signal (e.g., $A_1 = 0.5$, $A_2 = 0.5$) case. We surveyed and selected cases 1-4 based on knowledge of the phase behavior of four-quadrant inverse tangent.

As shown in Fig. 4, case 1 shows the best contrast even though it has the same initial phase difference as case 2. This is because when changing the fill factor coefficients, the calculated phase in case 1 crosses the -π/π border which introduces a 2π jump. This jump is a computational consequence, but its addition allows for better differentiating the two signals at mixed situation. On the contrary, the phase value in case 2 changes monotonically from π to π/2, there is not a dramatic phase jump. These differences are shown graphically in 4(b). Although cases 3 and 4, these have a larger initial phase difference than case 1 they exhibit problems around the 50% fill factor due to the fact that the summation of two sinusoidal signals with a π phase step always returns one of two phase values (Φ_1 or Φ_2). Because of the unbalanced fill factor, the summation of $I_{particle}$ and $I_{background}$ is just one of the two phases but with smaller amplitude. Near 50 % fill factor the amplitude of the sinusoidal signal gets small enough to where noise from the environment or sensor itself may disturb the result. The uncertainty in the calculated result makes cases 3 and 4 not suitable for AOI. It is worth noting that we are interested in making high contrast phase results to develop a reliable AOI method rather than precise phase retrieval. In this simulation study, we used the π phase shift input and 2π phase retrieving calculation (four-quadrants inverse tangent). So the phase retrieved results in Fig. 4 are not exactly match with the Table 1 input values.

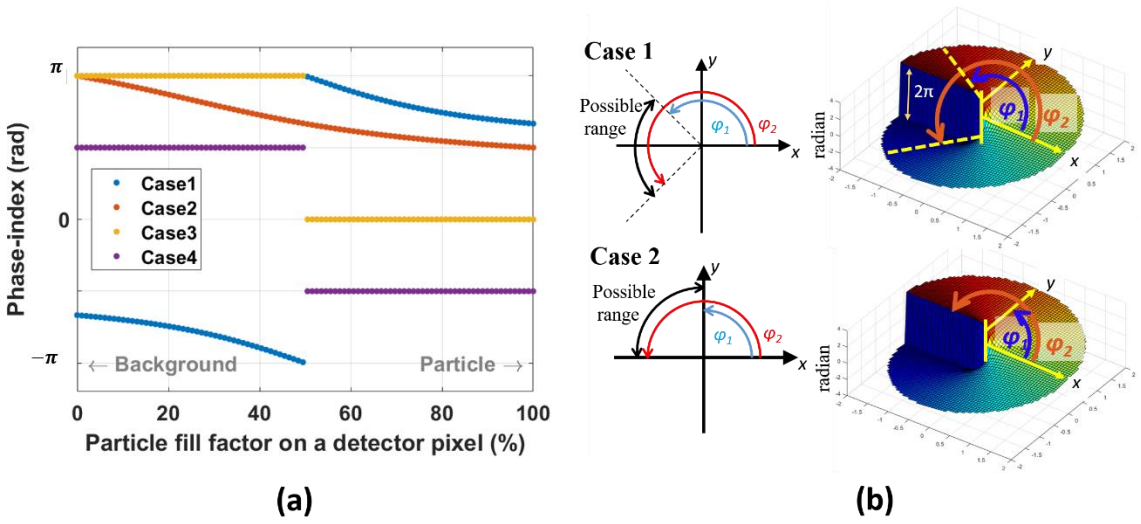

Figure 4. The case study of the representative phase steps. (a) Phase trend along with the fill factor variation. Having a big contrast at the pure signal (0 % and 100 %) is an essential requirement. The high contrast near 50% fill factor is a superb benefit of the MDFI coming from initial phase choice strategy. (b) The schematic diagrams of phase jumping behavior at the -π/π border. This specialty makes the huge contrast at the particle boundary which is blurry at the DFI test.

3. PERFORMANCE EVALUATION

The four cases of MDFI and traditional DFI were tested and evaluated. Off-the-shelf three-point emitting LEDs (Cree LEDs, XHP 35) and camera (Pointgrey, FL3-U3-13Y3M-C) were used for a normal DFI setup. For the MDFI background signal, we used a Dell 1097FP monitor, however it doesn't necessarily need to be a monitor a monochrome display with brightness control is also fine. A laptop controlled all hardware, measured and processed the data.

The camera and UUT (unit under test) distance is 55 cm and the camera lens is zoomed to fill the field of view of the camera with the sample. The sample is an aluminum coated first surface mirror (8 cm x 8 cm) and polycrystalline particle spray (Struers, DP-Spray P 35 µm) was used to deposit equal-sized particles (~35 µm) on the surface (Fig. 5). With this layout, the single pixel of the camera corresponds to an 80 um x 80 um area which is larger than the deposited particles. A defect size smaller than the camera system resolution is not an easy test case. However, the scattered light from the small particles was bright enough to be recorded on the sensor pixels, therefore the phase information could be recorded. We are not claiming this is a super resolution test, but MDFI will still show a blurred particle image that confirms the existence of a defect.

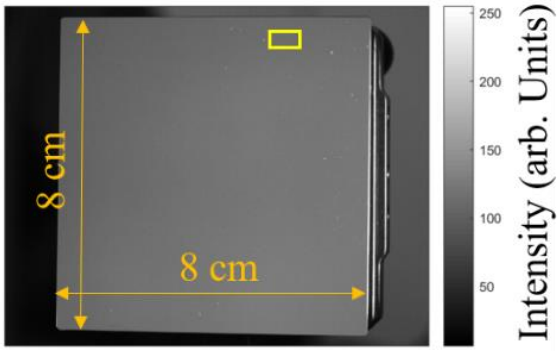

Figure 5. Captured Image of the sample. The yellow box indicates the evaluated area. The entire surface data shows us more than 1000 particles and it not easily seen by humans and checked the validation. The test is implemented for entire surface and the yellow box area only used to display in this paper. So, the small area test is identical to the entire surface test and also makes counting particles easier. MDFI is not limited to a certain test size once a camera can capture it.

As shown in Fig. 6, case 1 provides a sharp edge of the particle and better contrast ratio than other casess while cases 3 and 4 have a blurred boundary similar to traditional DFI. Case 2 failed to detect the particles because the poor SNR described earlier. These results clearly demonstrate that MDFI works properly and the selected initial phase steps follow theory.

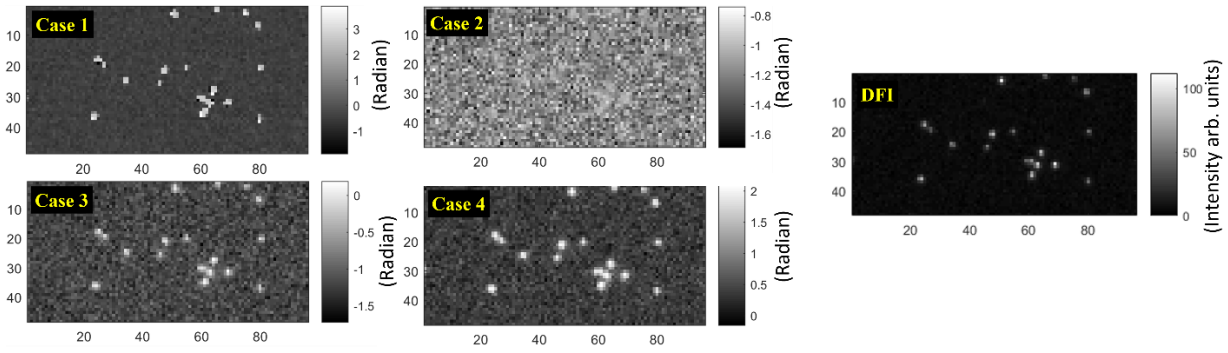

Figure 6. Test results of the MDFI and DFI. The color scale is normalized by the peak to valley values of the images.

4. AOI PERFORMANCE EVALUATION

Reliability is the most important attribute for an AOI to be applicable in the industry as false positives and true negatives of defects directly correlate to losses in time and money. In order to validate the reliability of MDFI, we tested the AOI testing using MDFI case 1 alongside DFI. Both methods were tested 10 times and the statistical values were evaluated.

The AOI algorithm found the positions and sizes of the particles without human help and made statistical tables. A fixed criteria was used to determine the existence of the particles and the criteria were adjusted to yield the best result for both methods respectively. All parameters including camera gain and LED brightness are set to have the best performance before the AOI test and once it starts all data processes are done automatically.

To normalize the evaluation, we used the same number of images for both methods because a single image averaged from multiple images removes the random noise giving more consistent data. MDFI used 10 snaps × 8 modulations (8 bright scales is adapted to have sinusoidal intensity variation), while DFI used 40 snaps × 2 (for the LED on and off). Fig. 7 shows the single-trial results after optimizing for best results. We reversed the intensity images for AOI algorithm. With the adjusted brightness, both results show clearly distinguishable particles. However, the MDFI still shows crisper particle edge.

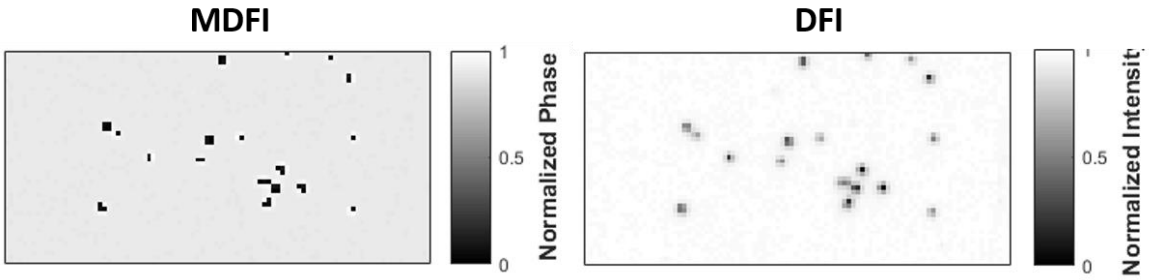

Figure 7. AOI single test results. After optimizing parameters, the final results show more clear particles image in both cases.

Once we found the best parameters for both methods, we took 10 measurements and the AOI calculated the statistical result maps (Fig. 8). In accordance to our theory, MDFI creates more reliable and consistent inspection results. DFI failed to detect three particles over the 10 measurements, two are missed completely and one was only detected 40 % of the time. For these same particles, MDFI shows 100 % and 90 % detection rate respectively.

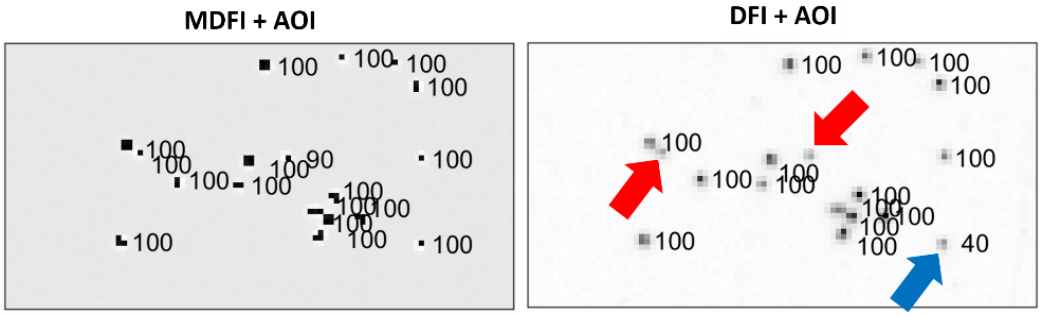

Figure 8. Fully automated AOI statistical results from 10 measurements. In the DFI results, two particles were missed completely (red arrow) and one was partially missed (blue arrow).

5. INSTANTANEOUS TEST

In the context of mass production in industry, time is money. MDFI requires image(s) at each phase step so it has a longer acquisition time than DFI which needs just two images for turning on and off. In order to overcome the time advantages DFI offers, we developed an instantaneous MDFI (iMDFI) using color multiplexing. To upgrade the experimental setup from MDFI to iMFDI, the monochrome camera and light sources simply need to replace with a color camera and color controllable sources. We opted to project red from the LED and blue from the monitor to have distinct color orthogonality on the camera color sensor. The single image is then decomposed into each of the color channels. In order to make the required phase data, we applied the phase wrapping computational image process method shown in Fig. 9.

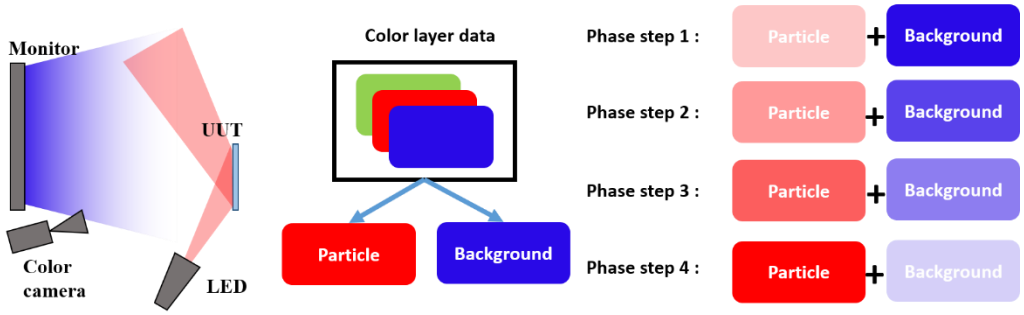

Figure 9. Schematic diagram of iMDFI setup and computational image process. The decomposed red and blue channel data contained the particle and background information, respectively. The varying amplitude (A_1 and A_2 equation in 2 and 3) is applying to each color channel and combined to have the phase such as MDFI. After that, the following data process is identical. By adjusting the amplitude, the broadcast phase is controlled to have good contrast.

The previous MDFI setup has to adjust the displayed (shone) phase during the data acquisition and the number of phase steps is limited by hardware properties (such like grayscale of the monitor and LED driver). With the addition of color multiplexing a single image may be taken, where the phase stepping may be applied in post processing once the images color channels have been decomposed. This is done by computationally varying the amplitude from each channel, red and blue, then computing the net phase trend given by equation 1. Now the phase stepping may be done instantaneously, relative to its predecessor, and the number of allowable phase steps is theoretically infinite as it is no longer hardware limited.

Information is leaked between color channels because the color camera doesn't have perfect color orthogonality. However, thanks to the robustness of phase calculations, this leaking does not disturb the inspection quality. Realistically, DFI cannot be implemented instantaneously because the camera has to take two images during the source is on then off, so there is no way to introduce color multiplexing in DFI hardware layout. However, if we use the iMDFI setup (especially the monitor signal), and mimic the computational image process of iMDFI, it is also possible to mimic a single image taken from a DFI test. For completeness, the instantaneous DFI (iDFI) results are presented alongside iMDFI results. The post processed phase data provided the same benefits as the original, time consuming MDFI, and iMDFI maintains a better detection rate and crisper boundaries than iDFI as shown in Fig. 10.

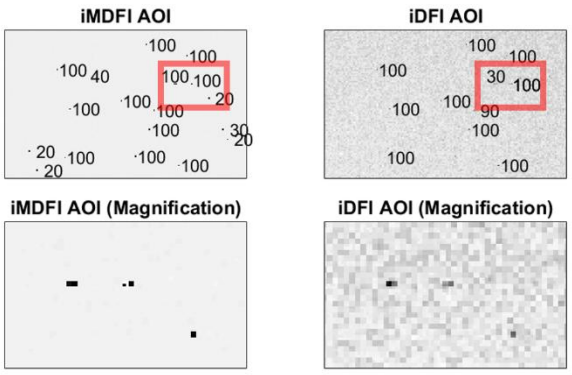

Figure 10. The Instantaneous MDFI and DFI results. The red boxes in top row plots show the position of the magnification view area. As we discuss in the previous chapter, the phase based calculation (iMDFI) has even distributed background and clear distinguishable particle. This help to make reliable inspection results.

6. CONCLUSION

Dark Field Illumination is a well-known classical method used for optical inspection. We improve its applications by introducing phase information and color multiplexing. The modulated intensity with distinguishable phase information demonstrates reliability in inspection and validation. To improve upon the longer acquisition time, the instantaneous method was developed; where its post-process phase wrapping calculation requires only one picture. This reduces acquisition time by a factor of N (number of total phase steps), 8 in our case since we used 8 steps in MDFI our tests, without sacrificing reliability or quality. We hope that this method provides a solution to the Automated Optical Inspection of surfaces (e.g. substrates or masks) in the industry environment.

Acknowledgment: This research was made possible in part by the II-VI Foundation Block-Gift Program, the Technology Research Initiative Fund Optics/Imaging Program, and the Friends of Tucson Optics Endowed Scholarships in Optical Sciences. The authors wish to thank Spectral Optics for the use of their equipment.

REFERENCES

[1] H. Golnabi and A. Asadpour. "Design and application of industrial machine vision systems," Robotics and Computer-Integrated Manufacturing **23**, 630-637 (2007).

[2] K. Harding, "Handbook of Optical Dimensional Metrology," Chap 2., CRC Press, (2013).

[3] E. N. Malamas, E. G. M. Petrakis, M. Zervakis, L. Petit, and J. D. Legat, "A survey on industrial vision systems, applications and tools," Image and Vision Computing **21**(2), 171-188 (2003).

[4] S. H. Gage, "Modern dark-field microscopy and the history of its development," Transactions of the American Microscopical Society **39**(2), 95-141 (1920).

[5] M. Feldman and O. W. Lynn, "Inspection system utilizing dark-field illumination," U.S. Patent 4,595,289 (Jun 17, 1986).

[6] G. Addiego, "Automated specimen inspection system for and method of distinguishing features or anomalies under either bright field or dark field illumination," U.S. Patent 5917588A (Jun 29, 1999).

[7] K. Maslov, G. Stoica, and L. V. Wang, "In vivo dark-field reflection-mode photoacoustic microscopy." Optics Letters **30**(6), 625-627 (2005).

[8] P. T. Goedhart, M. Khalilzada, R. Bezemer, J. Merza, and C. Ince, "Sidestream Dark Field (SDF) imaging: a novel stroboscopic LED ring-based imaging modality for clinical assessment of the microcirculation," Optics Express **15**(23), 15101-15114 (2007).

[9] H. Choi,J. M. Kam, J. D. Berkson, L. R. Graves, and Dae Wook Kim, "Modulated dark-field phasing detection for automatic optical inspection," Optical Engineering **58**(9), 092603 (2019)